Transparency Built-in

Energy Consumption and Cost Estimation for Additive Manufacturing

Martin Baumers, Chris Tuck, Ricky Wildman, Ian Ashcroft, Emma Rosamond, and Richard Hague

Keywords:

digital supply chain
energy consumption
industrial ecology
manufacturing process
rapid manufacturing
rapid prototyping

Summary

The supply chains found in modern manufacturing are often complex and long. The resulting opacity poses a significant barrier to the measurement and minimization of energy consumption and therefore to the implementation of sustainable manufacturing. The current article investigates whether the adoption of additive manufacturing (AM) technology can be used to reach transparency in terms of energy and financial inputs to manufacturing operations.

AM refers to the use of a group of electricity-driven technologies capable of combining materials to manufacture geometrically complex products in a single digitally controlled process step, entirely without molds, dies, or other tooling. The single-step nature affords full measurability with respect to process energy inputs and production costs. However, the parallel character of AM (allowing the contemporaneous production of multiple parts) poses previously unconsidered problems in the estimation of manufacturing resource consumption.

This research discusses the implementation of a tool for the estimation of process energy flows and costs occurring in the AM technology variant direct metal laser sintering. It is demonstrated that accurate predictions can be made for the production of a basket of sample parts. Further, it is shown that, unlike conventional processes, the quantity and variety of parts demanded and the resulting ability to fully utilize the available machine capacity have an impact on process efficiency. It is also demonstrated that cost minimization in additive manufacturing may lead to the minimization of process energy consumption, thereby motivating sustainability improvements.

Introduction

According to data from the World Resources Institute, industrial energy consumption, industrial processes, and transportation contributed 33.3% of world greenhouse gas emissions in 2005 (Herzog 2009). Researchers argue that the limitation of carbon emissions associated with energy consumption in manufacturing will become necessary (Jovane et al. 2008; Westkämper et al. 2000). Predictions suggest, however, that energy consumption occurring in industry will grow faster than in any other sector until 2050 (Taylor 2008). Therefore it appears critical to seek new ways to reduce the energy consumed in the mass production of goods.

A precise understanding of the emissions associated with manufacturing processes is fundamental regarding decision making toward sustainability. The measurement of such

Address correspondence to: Martin Baumers, Wolfson School of Mechanical and Manufacturing Engineering, Loughborough University, Loughborough, LE11 3TU, UK.
Email: m.baumers@lboro.ac.uk

DOI: 10.1111/j.1530-9290.2012.00512.x

Volume 17, Number 3

emissions forms an important area of research in the field of industrial ecology, where a variety of methods are employed to analyze the interactions between human activity and the environment (Gößling-Reisemann 2008). The quantification of carbon emissions, referred to as "carbon accounting," requires a precise understanding of the energy flows associated with production processes (Vijayaraghavan and Dornfeld 2010) and the emission characteristics of the local power grid (Jeswiet and Kara 2008).

The minimization of resource consumption during manufacturing is a major goal in "design for environment" methodologies (Telenko et al. 2008). However, the long supply chains characterizing modern manufacturing, routinely spanning the globe, may make recording the resource flows difficult; this leads to the conclusion that "if you can't measure, you can't manage" (Foran et al. 2005).

As discussed by Kellens and colleagues (2012), data on manufacturing process productivity, energy consumption, consumables usage and emissions are fundamental to the ecological impact occurring during manufacturing. Due to the carbon dioxide (CO_2) emissions associated with electric power usage (Jeswiet and Kara 2008), the measurement of process energy consumption forms a cornerstone in life cycle analyses of the impact of products. Specifically, such measurements contribute to inventory analysis, which compiles all energy and material flows throughout the life cycle (Jiménez-González and Overcash 2000).

In the current article, the PAS2050:2011 (British Standards Institution 2011) framework serves as an example for life cycle analysis methodologies. PAS2050:2011 allows two types of analyses: a "cradle-to-grave" assessment that surveys the major stages occurring in a product's life cycle, made up of raw material generation, manufacture, distribution, use phase, and a final disposal or recycling stage. A more limited "cradle-to-gate" analysis focuses on the stages of raw material extraction and manufacturing.

The term additive manufacturing (AM) refers to the use of a collection of electricity-driven technologies capable of combining materials to manufacture complex products in a single digitally controlled process step, entirely without molds, dies, or other tooling. As a one-stop manufacturing process, AM may be adopted to replace traditional process chains, which are often marked by length and complexity (Tuck et al. 2007). The current article demonstrates that where the creation of part geometry is concentrated into a single production step, measurement of the energy flows used to transform raw material into finished (or nearly finished) components is greatly simplified. Thus the adoption of AM may also ease the measurement of process energy consumption and carbon accounting.

The label "additive manufacturing" has been adopted to reflect the layer-by-layer fashion in which AM machinery incrementally builds up products and components (see ASTM 2010). This is in contrast to the various methods of conventional manufacturing, which commonly employ subtractive processes (such as machining) that operate by removing material, or formative techniques (such as injection molding) that give shape to a raw material. The emergence of AM has led to new possibilities in product design (Hague et al. 2004; Hollington 2008) and permits novel digital supply chain configurations (Tuck et al. 2007).

A major AM technology variant used to manufacture metal components is direct metal laser sintering (DMLS). The current article analyzes the EOSINT M270 platform (EOS GmbH 2010), belonging to the class of DMLS technology. DMLS operates as follows: a three-dimensional representation of the product geometry is digitally cut into discrete slices. These slices are then transmitted to the DMLS machine, which recombines them in a layer-by-layer sequence. To this end, the EOSINT M270 selectively scans the surface of a metal powder bed with a 200 watt (W) fiber laser, effectively creating a thin, planar slice of solid part geometry.[1] Once the sintering of the layer is complete, a fresh 0.02 millimeter (mm) increment of metal powder (in this case stainless steel) is deposited and the sintering of the next layer commences.[2] This cycle is repeated until the build is complete. It is important to note that the EOSINT M270 is capable of creating multiple components per build. To allow the dissipation of thermal energy into the frame of the DMLS machine, all produced parts are constructed onto a removable build plate, which also forms the floor of the build volume. Moreover, the process may require auxiliary structures for island features or undercuts relative to the AM system's vertical axis. Commonly a wire erosion machine is used to harvest the parts from the build plate after the build has been completed.

Comparing AM to conventional manufacturing processes, two main advantages have been identified (Tuck et al. 2008): first, AM may enable production without many of the constraints on part geometry that apply to other techniques. This may lead to products featuring a complex geometry and to the integration of multiple functions into single components. Second, AM allows the manufacture of highly customized products in small quantities at a relatively low cost. At the current state of technology, however, the routine application of AM is still hampered by a number of limiting factors (Ruffo and Hague 2007):

- limited material suitability,
- diminished process productivity,
- problems with dimensional accuracy,
- poor surface finish,
- repeatability issues, and
- uncompetitive production cost at medium and large volumes.

In response to the technology's current shortcomings in terms of dimensional accuracy and surface finish, metallic AM products are often subject to light finish machining (Cormier et al. 2004) or shot blasting (Mazzioli et al. 2009).

While enabling complete ex post transparency of the manufacturing input flows, AM's ability to produce multiple components contemporaneously poses a number of problems for the estimation of energy consumption and production cost (Ruffo and Hague 2007). The novelty of the current article lies in the

provision of a combined energy consumption and cost model that results in valid estimates for the AM process. An ability to calculate accurate estimates of the financial cost of manufacturing operations is vital for process selection. Further, the ability to accurately model the energy inputs is very valuable in the determination of the ecological impact associated with process energy consumption, and ultimately the environmental footprint of products. Other nonnegligible factors shaping the environmental impact of AM are raw material consumption and process emissions; these further factors are not assessed in the current article.

However, for a conclusive appraisal of the total environmental impact associated with the adoption of a manufacturing technology, all stages of the product life cycle need to be assessed, ranging from raw material generation to a final recycling or disposal stage. Therefore the results of the current study should not be used to directly compare the environmental performance of AM against other processes. Moreover, process selection is very likely to also influence optimal design and material specifications (Boothroyd et al. 1994). These factors also affect the environmental performance of a product or part. The argument against such "ceteris paribus" analyses of AM against conventional technologies is elaborated by Baumers and colleagues (2011).

Material and Methods

To exploit the transparency inherent in AM as a one-stop, electricity-driven technology, a novel tool for the combined estimation of electric and monetary inputs is implemented. As argued below, the treatment of AM as a parallel manufacturing technology (Ruffo et al. 2006a) further makes the incorporation of build volume packing functionality necessary. The discussed approach builds on a novel, voxel-based time estimation technique providing input for an equally novel energy consumption estimator. Finally, financial cost estimates are obtained from an activity-based costing (ABC) framework of the type proposed by Ruffo and colleagues (2006a). The development of an estimation tool thus builds on three streams of AM-related literature: (1) the estimation of build time for additive techniques; (2) cost modeling, usually carried out for particular AM technology variants; and (3) the existing work reporting on AM energy consumption. Following a brief discussion of relevant items in the literature, this section describes the used energy consumption measurement methodology, introduces the various test geometries manufactured during a series of build experiments, and presents the cost data collected. The implementation of the estimation tool is discussed in a separate section.

Build Time Estimation

Commercially available rapid prototyping software packages contain build time estimation functionality (Campbell et al. 2008), as do the machine software suites sold in bundles with additive systems (Ruffo et al. 2006b). Offering a framework for the classification of AM build time estimators, Di Angelo and Di Stefano (2011) argue that the existing approaches can be divided into "detailed-analysis" methods based on knowledge of the inner workings of AM systems and "parametric" methods informed by data on a set of process characteristics such as layer thickness, hatch distance, and laser scan velocity. A body of research exists on build time estimation for the AM technology variant laser sintering (Choi and Samavedam 2002; Pham and Wang 2000; Ruffo et al. 2006b). In comparison, published work on metallic AM build time estimation is scarce. Munguia (2009) suggests that this may be due to competitive behavior exhibited by AM control software authors or due to idiosyncrasies in the postprocessing of metal parts. Munguia also presents an artificial neural network time estimation approach for metallic AM.

Additive Manufacturing Cost Modeling

Build time estimation forms the starting point for AM production cost estimation models in the literature (Alexander et al. 1998; Byun and Lee 2006; Campbell et al. 2008; Ruffo et al. 2006b). Ignoring "ill-structured costs" (Son 1991) arising from build failure, idleness, and inventory, Ruffo and colleagues (2006a) propose an AM costing model viewing the total cost of a build, C_{Build}, as the sum of all direct raw material costs and the indirect costs (equation 1). The direct costs are obtained by multiplying the mass of deposited material, M_{Build}, by the cost of the raw material, $C_{Material}$, measured in pounds sterling (£) per kilogram (kg).[3] The indirect costs are calculated by multiplying the total build time, T_{Build}, by an indirect cost rate, $\dot{C}_{Indirect}$ (measured in £ per second):

$$C_{Build} = M_{Build} \times C_{Material} + T_{Build} \times \dot{C}_{Indirect}. \quad (1)$$

An estimate of cost per part, C_{Part}, is then calculated by dividing C_{Build} by the number of parts contained in the build, n_{Build}. Ruffo and Hague (2007) acknowledge that this method is only applicable to builds containing multiple instances of the same part—a premise that is quite alien to the idea of AM being used to flexibly build different parts in parallel.

Furthermore, Ruffo and Hague (2007) note that "in reality manufacturers set every build with the highest packing ratio possible," indicating an incentive to completely fill build volumes with products, potentially by selling available build volume space to external bidders. This, in turn, suggests that AM cost models relying on deliberately unused build volume capacity (e.g., Ruffo et al. 2006a) describe situations of nonminimal cost. The convention that cost functions and models exclusively describe configurations in which the highest possible quantity of output is produced with the used inputs (in this case capital) is fundamental. Configurations that satisfy this requirement are defined as being technically efficient (Else and Curwen 1990). With respect to the possibilities afforded by AM, it is doubtful that models constructed by deliberately leaving capacity unused satisfy this requirement.

It is interesting to note that the AM costing model presented by Hopkinson and Dickens (2003) does not fall into the trap of describing cost relationships on the basis of unutilized machine capacity. By concentrating on high-quantity AM, in which a single design is made at maximum capacity for a year, Hopkinson and Dickens (2003) produce cost estimates on the basis of technical efficiency, albeit for the single product case. Implicitly supporting the argument made above, the cost functions shown by Hopkinson and Dickens (describing the relationship between unit cost and production volume) are flat, hence production cost is viewed as independent of quantity.

Previous Work on Additive Manufacturing Energy Consumption

Subtractive processes, such as machining, form an important substitute technology to metallic AM. They are the subject of a number of studies assessing the relationship between energy inputs and process parameters (Dietmair and Verl 2009; Kara and Li 2011; Rajemi et al. 2010; Sarwar et al. 2009). For the analysis of electrical energy requirements of various manufacturing processes, Gutowski and colleagues (2006) propose a general framework using the concept of exergy. Moreover, Gutowski and colleagues report results reached by Morrow and colleagues (2004) on the process energy consumption of the AM technology variant direct metal deposition (DMD).

Mognol and colleagues (2006) report the energy usage of a now obsolete version of the DMLS system investigated in this research, analyzing the energy inputs to single-part build experiments. Reporting a mean real power consumption of 4.00 kilowatts (kW), Mognol and colleagues conclude that part orientation affects total energy consumption due to the large effect of a part's Z-height on overall energy consumption.[4] For the production of a test part with a volume of 8.00 cubic centimeters (cm^3), the authors cite a minimum total energy consumption of 115.2 megajoules (MJ).[5] Kellens and colleagues (2010) investigate the energy consumption of the Concept Laser M3 linear selective laser melting system, which is technologically closely related to the investigated DMLS system. For the production of a batch of parts with a mass of 409 grams (g), a total energy consumption of 39.60 MJ is reported, which allows the calculation of a specific energy consumption of 96.82 MJ/kg of material deposited.[6] This corresponds to the specific energy consumption rates reported by Baumers and colleagues (2010) for the two metallic AM technology variants electron beam melting (EBM) and selective laser melting (SLM). Specific energy consumption of the EBM platform is measured at 61.20 MJ while the SLM system consumes 111.60 MJ/kg of material deposited. Corresponding to these results, Strutt (1980) notes that laser-based manufacturing processes may be much less energy efficient than comparable systems utilizing an electron beam, due to lower energy transfer efficiency.

Compared to the AM energy consumption results presented above, the energy consumption cited by Morrow and colleagues (2007) for the AM technology variant DMD is much greater, where a specific energy consumption of 7708 MJ/kg of raw material deposited is reported. Moreover, Morrow and colleagues combine the data on DMD energy consumption with the energy embedded in the H13 steel raw material powder, producing a "cradle-to-gate" variant of a life cycle analysis. However, due to the very low deposition rate setting of 0.01 grams per second (g/s), the results reached by Morrow and colleagues appear problematic in terms of efficient DMD technology usage.

While energy consumption estimators analogous to AM cost estimators are not documented, one result from the AM cost estimation literature is transferrable to energy inputs: overall energy consumption is affected by capacity utilization (Baumers et al. 2010). It is also likely that the mix of parts in an individual build influences the energy efficiency of the process.

Empirical Data Used for Modeling and Validation

To provide the empirical data, a series of build experiments was performed on the EOSINT M270 DMLS system with factory settings. This set of default operating parameters includes the following:

- layer thickness of 0.02 mm, set in conjunction with the used stainless steel raw material (grade 17–4 PH) in powder form;
- scan path overlap of 0.5 mm;
- hatch scan strip width of 10 mm;
- contour scanning: scan speed of 700 mm/s, 60 W nominal beam power, 40 W for downward-facing surfaces;
- outer skin scanning: scan speed of 1,000 mm/s, 195 W nominal beam power; and
- postcontour scanning: scan speed of 1,000 mm/s, 195 W nominal beam power.

For the energy component in life cycle inventory analyses, the variable of interest is mean real power consumption per measurement interval. The energy inputs during these build experiments were recorded using a Yokogawa CW240 digital power meter attached to the main power connection, in the same configuration used by Baumers and colleagues (2010). This setup takes into account the energy used to provide the nitrogen (N_2) required to shield the process from oxygen as the N_2 generator is attached to the system's power supply. To simplify this analysis, the impact of the used compressed air (supplied by the local facility) is ignored. The EOSINT M270's data sheet (EOS GmbH 2010) suggests a nominal compressed air requirement of 20 cubic meters per hour (m^3/h) at 7,000 hectopascals (hPa). In total, four build experiments were undertaken.

Data Collection Experiment

The first experiment was performed to collect energy consumption and build time data. To achieve this, a specifically designed test part (shown in figure 1a) was built directly on the build platform. To ensure sufficient data resolution, mean real power consumption was logged in 100 millisecond (ms) intervals.

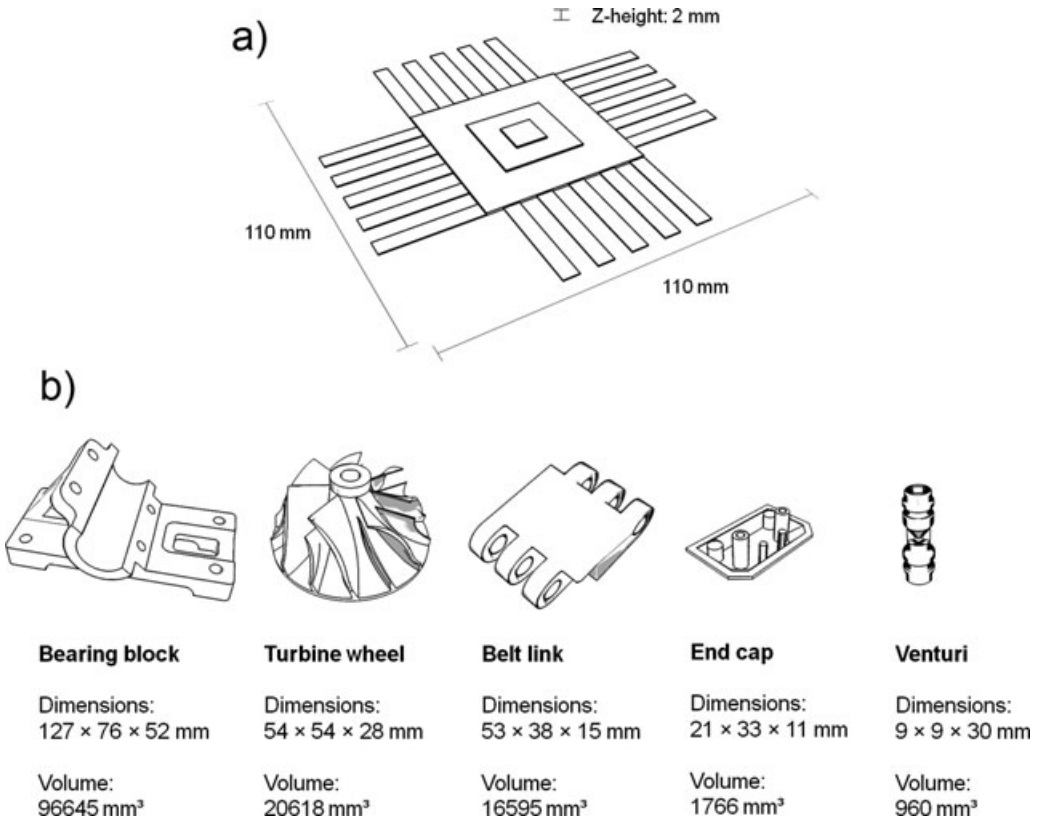

Figure 1 Power monitoring test part and a basket of sample parts, with dimensions in millimeters (mm).

Validation Experiments

Three further experiments were conducted to validate the combined energy consumption and time estimator. This included a multipart build at full machine capacity, as well as two single-part builds to test model accuracy in single-part configurations. As cumulative energy consumption values were in the foreground in these experiments and the power meter logs the largest number of power-related variables in this setting, the data were recorded with a time resolution of 1 s. To populate the workspace, emulating a realistic application of AM, a basket of five test parts was defined (shown in figure 1b). The composition of this basket was chosen to be representative of the products commercially manufactured using DMLS and to reflect variation in product size, geometry, and application.

The energy consumed by the separation of the parts from the removable build plate in an ancillary wire erosion process was also monitored. The wire erosion process operates by passing an electrically charged brass wire along the surface of the build substrate from one side of the build plate to the other. The energy usage of the wire erosion process depends heavily on the cutting time, which in turn depends on the length of the interface connecting the parts to the substrate. Experiments show that the amount of energy used in the wire erosion process tends to be independent of part geometry and build volume utilization. The mean real power consumption of the wire erosion process is measured at 3.96 kW, which is lower than the values observed for this technology by Gutowski and colleagues (2006), ranging from 6.60 kW to 14.25 kW. This may be due to the fact that the entry-level system used (an Agie Charmilles CUT20) is comparatively small.

On the CUT20, the separation of a full build of parts from the metal substrate is observed to take approximately 600 minutes (36,000 s). Thus, for each build, the energy investment for the wire erosion process is assumed to be constant at 142.46 MJ. The estimator applies this amount of energy consumption to the energy consumption estimate of every build, irrespective of build configuration. Moreover, the wire erosion process for full builds and single-part builds is thus treated identically, which may be a further simplification. Please note, however, that this element of energy consumption is not included for the validation of the estimator.

Cost Data

Cost estimation is based on a combination of data published by Ruffo and colleagues (2006a) and expenditure data provided by the EOSINT M270 machine operator, Bentley Motors, in Crewe (UK). For consistency, all cost data are reported in 2010 pounds sterling (£), and have been converted where necessary. Table 1 presents the data informing the cost model specified for the EOSINT M270, including the cost arising from the ancillary wire erosion process.

Table 1 Direct and indirect cost elements (adapted from Ruffo et al. 2006a)

Cost elements			*Cost elements (cont.)*		
Production overhead			*Equipment*		
Rent, building area cost	4.53	£/h	AM equipment and wire eroder	8.00	years
			Hardware and software	5.00	years
Administration overhead					
Hardware purchase	1,670.27	£	*Machine costs*		
Software purchase	1,670.27	£	Machine purchase	364,406.80	£
Hardware cost/year	334.05	£	Machine purchase cost per year	45,550.85	£
Software cost/year	334.05	£	Maintenance cost per year	22,033.90	£
Consumables per year	1,113.52	£	Machine consumables per year	2,542.37	£
Total administration overhead	0.31	£/h	Wire erosion machine purchase	55,000.00	£
			Total wire erosion costs per year	8,165.00	£
Production labor			Total machine costs per year	78,292.12	£
Technician annual salary	25,165.45	£	Total machine costs	15.66	£/h
Employer contributions	22.00	%			
Total production labor	6.14	£/h			
Utilization			**Total indirect costs per machine hour**	**26.64**	**£**
Utilization rate	57.04	%	**Direct cost for 17-4 PH powder/kg**	**78.81**	**£**
Annual machine operating hours	5,000.00	h	**Direct electricity costs per MJ**	**0.018**	**£**

Notes: £ = 2010 pounds sterling; h = hours; kg = kilograms; MJ = megajoules.

Implementation

To allow full flexibility and portability, the combined energy and cost estimation tool, including all subordinate functions such as workspace configuration and build time estimation, is implemented in C++ as a console application. The implementation was written using the free integrated development environment Dev-C++ (version 4.9.9.2).

Additive Manufacturing Build Volume Packing

While the cost model presented by Ruffo and colleagues (2006a) appears very useful for capital-heavy production processes such as AM, the requirement for technical efficiency implies that the available capacity should be fully utilized in the estimation of AM production cost. This problem is solved by including build volume packing functionality in the estimation tool, thereby producing acceptable build configurations from the basket of parts shown in figure 1b, ideally exhibiting a maximum level of capacity utilization.

Workspace packing approaches have been discussed in the literature in an effort to make AM more economical by automating this activity (Hur et al. 2001; Nyaluke et al. 1996). In the determination of packing strategies, part placement is usually determined by some optimization technique (Hur et al. 2001; Ikonen et al. 1997; Wodziak et al. 1994). For an efficient packing outcome, Hur and colleagues (2001) suggest using voxel approximations of part geometry to determine part placement and orientation, allowing nested configurations of parts in the build volume. To balance the performance of the build volume packing algorithm with resources available for its development, two decisions were made before developing the algorithm:

1. To achieve an efficient packing result, the algorithm was based upon rough voxel representations of the test parts (with a resolution of 5 mm). This effectively discretizes the problem of placing irregular and continuous geometries.
2. To allow the definition of different demand profiles faced by the AM user, the parts are inserted into the build volume in a fixed sequence that is determined exogenously. The algorithm ensures that at least one instance of each demanded part is included in the build volume.

The next step in the design of the packing algorithm is the selection of an evaluation criterion that is suitable for the wide range of different geometries and part sizes exhibited by the basket of test parts. The resulting implementation moves and rotates inserted parts such that centers of mass are as close together as possible, thereby producing a densely packed build configuration.

Due to the application of this approach to DMLS, where all parts are constructed on the base plate, part movement is limited to the x–y plane. Further, to facilitate the voxel representation of the parts and to avoid problems of anisotropic material properties occurring in metallic AM, part rotation is constrained to the vertical axis in discrete 90° steps.

Demand Profile Definition

An intertemporal production scheduling decision will usually mean that total demand for parts exceeds machine capacity available at a given point in time. This is modeled by allowing the total demand for parts to exceed available machine capacity, which may be interpreted as demand extending into the future. The construction of an energy and cost estimator

allowing for such excess demand in the multiproduct case can be facilitated by the definition of some order of precedence for k different parts. This can be interpreted as a measure of comparative urgency of the production of individual components. In a situation of demand exceeding the available capacity, this precedence order is likely to govern the composition of a build. Thus the demand profile faced by the AM user in this specification contains two elements: first, the demand level for each of the k parts, and second, an indication of the order of precedence. The instantaneous demand level measured in integer units for each of the k parts can be expressed as a k element vector **dd**, where $dd_i \in \mathbb{N}$,

$$\mathbf{dd} = [dd_1\ dd_2 \cdots dd_{k-1}\ dd_k]. \tag{2}$$

The assignment of an order of precedence to each of the k parts results in a vector **p** with k elements, where $\{p_i \in \mathbb{N} | 0 < p_i \leq k\}$ and $p_i \neq p_j$:

$$\mathbf{p} = [p_i\ p_2 \cdots p_{k-1}\ p_k]. \tag{3}$$

Build Time Estimation

Once the build configuration is determined by executing the build volume packing algorithm, the next step is to estimate build time, which forms a prerequisite for cost estimation (Munguia 2009; Ruffo et al. 2006b). The estimate for total build time, T_{Build}, is obtained by combining data from a hierarchy of elements of time consumption:

- fixed time consumption per build operation, T_{Job}, including, for example, machine atmosphere generation and machine warm-up;
- total layer dependent time consumption, obtained by multiplying the fixed time consumption per layer, T_{Layer}, by the total number of build layers l;
- the total build time needed for the deposition of part geometry approximated by the voxels. The triple Σ operator in equation (4) is used to express the summation of the time needed to process each voxel, $T_{\text{Voxel}\,xyz}$, in a three-dimensional array representing the discretized build configuration:

$$T_{\text{Build}} = T_{\text{job}} + (T_{\text{Layer}} \times l) + \sum_{z=1}^{z}\sum_{y=1}^{y}\sum_{x=1}^{x} T_{\text{Voxel}\,xyz}. \tag{4}$$

No allowance is made for build preparation and machine cleaning. It is felt that the time spent on these activities is difficult to measure and very much at the discretion of the machine operator. It could be argued that these activities take place during the 42.96% of nonoperational hours (as shown in table 1).

In the commercial setting surveyed, the EOSINT M270 is kept in a standby state when idle, except during holidays or maintenance, when it is switched off completely. In this standby state, the N_2 supply is shut down, with only the laser chiller, the control computer, and some secondary functions active. However, this configuration does not reflect energy-conscious technology usage. For energy consumption minimization, the system should be deactivated completely or as far as possible during inactive periods, perhaps through the addition of an energy-saving mode.

Energy Consumption Estimation

Total energy investment, E_{Build}, can be modeled similarly to equation (4). However, a purely time-dependent element of power consumption must be expected in the continuous operation of the AM machine. This is denoted by the energy consumption rate $\dot{E}_{\text{Time}}$ (measured in MJ/s), which is multiplied by T_{Build} to estimate total time-dependent energy consumption. Modeling $\dot{E}_{\text{Time}}$ as a constant reflects its interpretation as a mean baseline level of energy consumption throughout the build, originating from continuously operating machine components such as cooling fans, pumps, and the control system.

E_{Job} contains all energy consumption attributable to the build job, including energy consumed by the wire erosion process to remove the parts from the build plate. Analogous to build time estimation, E_{Layer} denotes fixed elements of energy consumption per build and layer, for a total number of layers, l. Further, the geometry-dependent energy consumption is obtained by adding all energy consumption associated with voxel deposition, $E_{\text{Voxel}\,xyz}$, throughout the discretized workspace. Please note that $E_{\text{Voxel}\,xyz}$ does not contain time-dependent power consumption. The empirical data on $E_{\text{Voxel}\,xyz}$ were obtained by monitoring machine energy consumption during scanning and then subtracting the energy associated with the energy consumption rate $\dot{E}_{\text{Time}}$. Thus E_{Build} can be modeled as follows:

$$E_{\text{Build}} = E_{\text{Job}} + (\dot{E}_{\text{Time}} \times T_{\text{Build}}) + (E_{\text{Layer}} \times l) + \sum_{z=1}^{z}\sum_{y=1}^{y}\sum_{x=1}^{x} E_{\text{Voxel}\,xyz}. \tag{5}$$

This energy consumption model should not be interpreted as showing how total AM energy consumption can be attributed to individual subunits of the platform. The specification was chosen to implement a voxel-based energy consumption estimator. Moreover, both the time and energy estimation implementations possess additional information on the real Z-height of the parts contained in the build. This approach is chosen to avoid large estimation errors arising from the inclusion of empty layers.

Cost Estimation

For the current research, an activity-based cost (ABC) estimator of the type devised by Ruffo and colleagues (2006a) is employed. The cost estimate for the build, C_{Build}, is constructed by combining data on the total indirect costs and

direct costs incurred, thereby providing a measure of "relatively well-structured" costs (Son 1991) ignoring costs arising from risk of failure, setup, waiting, idleness, and inventory. Indirect costs, expressed as a cost rate, $\dot{C}_{\text{Indirect}}$, measured per machine hour, contain costs arising from administrative and production overheads, production labor, as well as machine costs (including depreciation). As listed in table 1, the current research estimates the total indirect cost rate of operating the EOSINT M270 at £26.64 per hour. It is noteworthy that the system incorporates an N_2 generator, hence no protective gas from external sources is needed.

Unlike in the work by Ruffo and colleagues (2006a), two direct costs enter the total cost estimates: raw material costs and energy costs. Total raw material costs are calculated by multiplying the total weight w of all parts included in the build (including support structures) with the price per kilogram of the stainless steel 17-4 PH powder, $Price_{\text{Raw material}}$ (£78.81/kg). The expenditure for energy enters the model by multiplication of the energy consumption estimate, E_{Build}, with the mean price of electricity for the manufacturing sector in the UK, $Price_{\text{Energy}}$, currently around £0.018/MJ (according to DECC 2010). Thus the total cost estimate for the build, C_{Build}, can be expressed as

$$C_{\text{Build}} = (\dot{C}_{\text{Indirect}} \times T_{\text{Build}}) + (w \times Price_{\text{Raw material}}) + (E_{\text{Build}} \times Price_{\text{Energy}}). \quad (6)$$

Results

Performance of the Build Volume Packing Algorithm

A full-capacity build experiment was designed by executing the build volume packing algorithm with excess demand **dd** for all parts. In the configuration maintained throughout the current article, the precedence vector **p** is ordered according to part size. Thus the first entry in **p** is the largest part, the bearing block, and the fifth entry is the smallest part in the basket, the venturi pipe (as shown in figure 1b). The resulting full build configuration is shown in figure 2. Of the available 2,025 build volume floor voxels, 92.6% were occupied. A total of 85 parts were inserted, thus utilizing 19.78% of the used build volume cuboid (225 mm × 225 mm × 52 mm). This value includes the auxiliary structures needed to dissipate heat from the overhanging part geometry.

Model Specification

The final specifications of the time and energy estimators are obtained from a least squares regression of the time and energy consumption data recorded during the deposition of each layer of the power monitoring test part, using the area scanned per layer as the independent variable. As shown in figure 1a, the power monitoring part is of layered design, resulting in the four different time and energy consumption levels shown in figure 3.

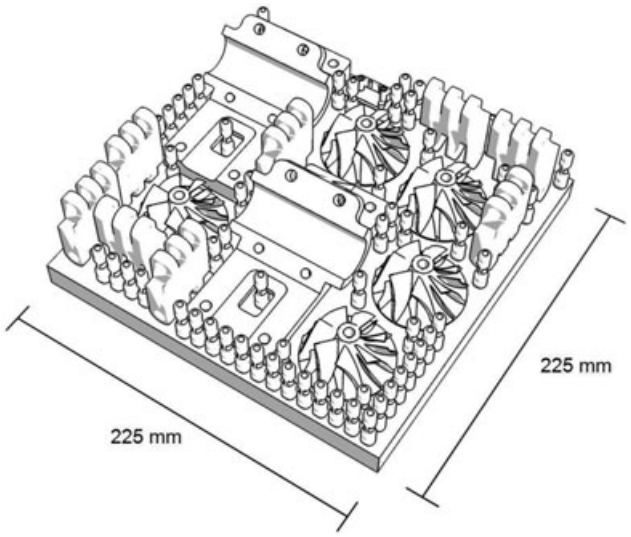

Figure 2 Full build configuration, with dimensions in millimeters (mm).

The obtained intercept parameters α_{Time} (10.82 s) and α_{Energy} (0.008 MJ) are multiplied by the number of layers in the build l in order to obtain layer-dependent time and energy consumption. The slope parameters expressing the time and energy attributable to the scanning of 1 mm^2 during the build, β_{Time} (0.0125 s) and β_{Energy} (0.000013 MJ), are then used in conjunction with the layer thickness lt (0.02 mm) and a measure of occupancy of each voxel to calculate total time and energy consumption per voxel, $T_{\text{Voxel}\,xyz}$ and $E_{\text{Voxel}\,xyz}$, respectively. The rate of occupancy (RO_i) in each voxel depends on the ratio of the volume of part i occupying this voxel (VP_i) and the volume of the voxel approximation for part i (VA_i):

$$RO_i = \frac{VP_i}{VA_i}. \quad (7)$$

Thus, for each (5 mm)^3 voxel in the position xyz holding 250 (= 5 mm/lt) layers and containing part i, the build time and energy consumption can be approximated:

$$T_{\text{Voxel}\,xyz} = \beta_{\text{Time}} \times 5^2 \times \frac{5}{lt} \times RO_i \quad (8)$$

$$E_{\text{Voxel}\,xyz} = \beta_{\text{Energy}} \times 5^2 \times \frac{5}{lt} \times RO_i. \quad (9)$$

This is combined with an estimated fixed time and energy consumption for machine startup, T_{Job} (63 s) and E_{Job} (142.58 MJ, including wire erosion). The startup process is very rapid on this system, as no system warm-up is required and the build chamber is continuously flooded with N_2 during build activity. It should be noted that E_{Build} also contains the time-dependent power consumption, obtained by multiplying the baseline energy consumption rate $\dot{E}_{\text{Time}}$ (0.0015 MJ/s) by T_{Build}. The

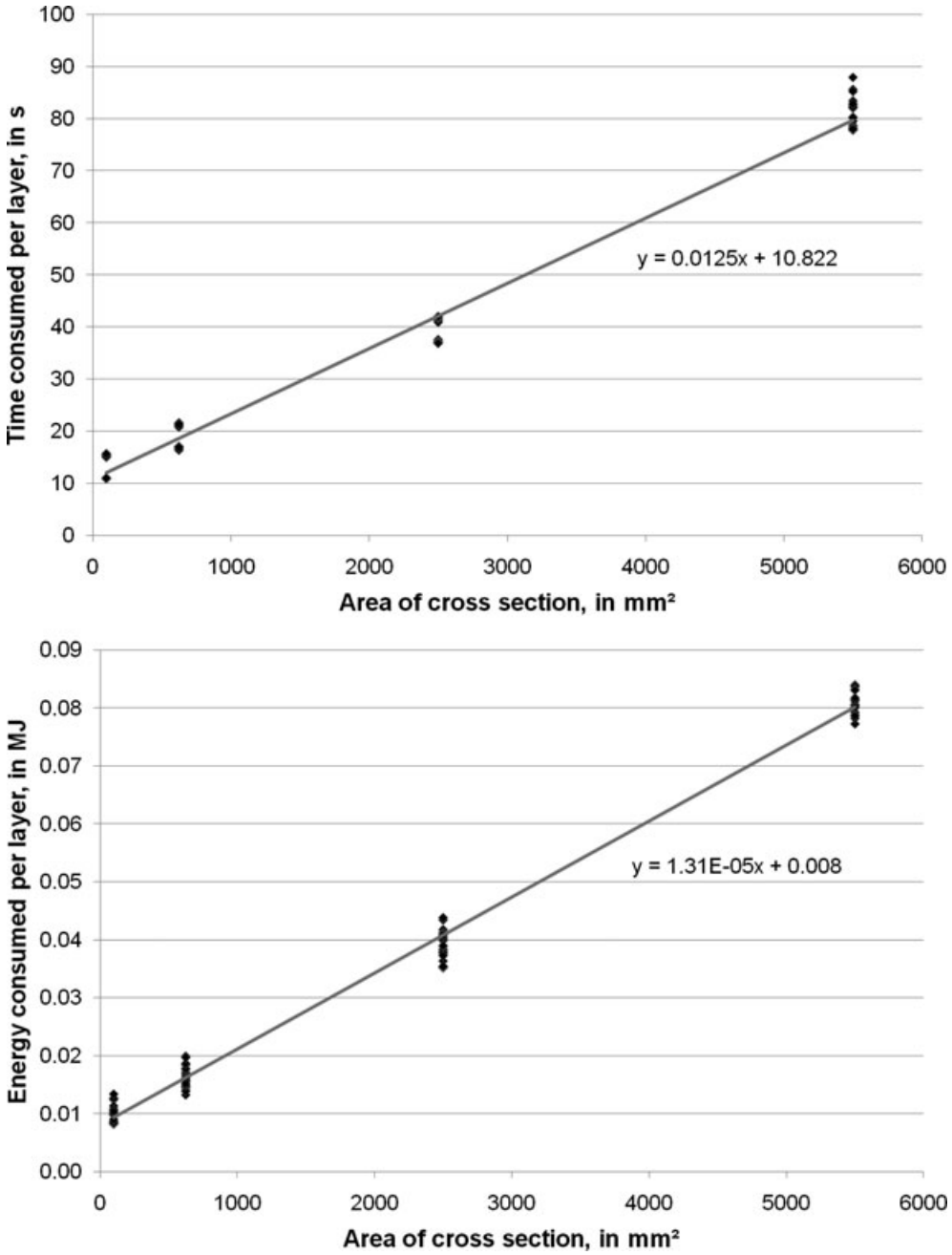

Figure 3 Regressing cross-section area against time and energy consumption, with dimensions in millimeters (mm), time in seconds (s), and energy in megajoules (MJ).

estimates of T_{Build} and E_{Build} are obtained as follows:

$$T_{\text{Build}} = T_{\text{Job}} + (\alpha_{\text{Time}} \times l) + \sum_{z=1}^{z} \sum_{y=1}^{y} \sum_{x=1}^{x} T_{\text{Voxel } xyz} \quad (10)$$

$$E_{\text{Build}} = E_{\text{Job}} + (\dot{E}_{\text{Time}} \times T_{\text{Build}}) + (\alpha_{\text{Energy}} \times l) + \sum_{z=1}^{z} \sum_{y=1}^{y} \sum_{x=1}^{x} E_{\text{Voxel } xyz}. \quad (11)$$

Validation of the Model

The time and energy consumption model specified in equations (10) and (11) can be validated by comparing the calculated estimates to the real time and energy consumption during three build experiments. Validation is performed for the full build at maximum machine capacity (shown in figure 2) and two builds of single components from the basket of sample parts, the bearing block and the turbine wheel. The results of the validation experiments and the corresponding estimates of T_{Build} and E_{Build} are presented in table 2. Note that the validation does

Table 2 Confronting the estimates with experimental results

Experiment	*Time consumed*	*Model time estimate,* T_{Build}	*Error*	*Energy usage*	*Model energy estimate,* E_{Build}	*Error*
Full build experiment	388,031 s	354,806 s	−8.56%	917.10 MJ	879.93 MJ	−4.05%
Single bearing block	93,302 s	92,338 s	−1.03%	215.48 MJ	223.13 MJ	3.55%
Single turbine wheel	31,224 s	28,504 s	−8.71%	72.73 MJ	66.80 MJ	−8.15%

Notes: s = seconds; MJ = megajoules.

not include the energy consumed by the ancillary wire erosion process, as the emphasis of this study is the core AM process. It should also be mentioned that some of the venturi parts had an incorrect orientation during the build, which, together with a design flaw, led to build failure for the affected parts in the final stages of the build. However, this was deemed to have had a negligible effect on the presented results.

The observed errors are likely to originate from the use of an idealized test part (figure 1) in the experiments that provided the data. Compared to other build time estimators (Campbell et al. 2008; Munguia 2009; Ruffo et al. 2006b; Wilson 2006), the mean absolute errors show that the developed time estimation functionality performs robustly.

Process Economics of the Full Build Experiment

The transparency characteristic of one-stop processes such as AM can be demonstrated on the basis of the full build experiment (as shown in figure 2). According to the experimental data (including the wire erosion process), the build consumed a total of 1059.56 MJ of energy. Using the specified cost model, C_{Build} is estimated at £3,218.87. Individual part shares of cost and energy usage are identified through their share of total product mass, which includes any support structures connecting the parts to the substrate (4.167 kg). Figure 4 thus shows the process energy consumption and production cost attributable to each part.

Discussion

The average cost functions for AM products proposed by Ruffo and colleagues (2006a) are downward sloping and stabilize asymptotically for large production quantities, suggesting that part quantity is a determinant of the process efficiency of AM. The current article argues that such considerations do not correspond to AM technology usage in practice, which is marked by AM users trying to operate their machinery as efficiently as possible by packing as many parts as possible into each build. Moreover, AM is used in a parallel mode of production that mixes multiple parts in varying quantities in each build. So if production quantity is not a useful determinant of AM production efficiency, what is?

The current article instead argues that the demand profile faced by the AM user has a significant impact. The combined energy consumption and cost estimator can be used to test the effect of different demand profiles. Table 3 lists eight such specifications, which are then used for cost and energy consumption estimation. The different demand profiles enter the estimator through the instantaneous demand vector **dd**. Note that demand for a particular part is allowed to exceed the available build volume capacity, and hence also exceeds the real number of parts that can be produced in one build (reported in brackets).

The concepts of full capacity utilization and technical efficiency are related, so this research takes the standpoint that technically efficient operation of the DMLS machinery does not imply the full exhaustion of the build volume capacity, which is an idealized situation that does not normally occur in practice. Rather, the position is taken that the nonexhaustion of the demand faced by the AM user signals technically efficient machine operation. Following this, the demand profiles A, B, C, E, F, and G satisfy the criterion. Moreover, table 3 lists the fraction of the build volume floor voxels that are occupied. It is noteworthy that for the builds deemed to be technically efficient, this fraction ranges from 50.07% (profile E) to 97.53% (profile G).

A possible criticism of this methodology is that by letting the packing algorithm select parts, the composition of the demand profile changes, eventually leading to a mismatch with what is demanded by the user. However, the presented model, based on the instantaneous demand profile **dd**, aims to reflect the situation at a particular point in time. Adding a temporal dimension would improve realism, but would also greatly increase model complexity.

By cumulating the total part volume resulting from each of the eight demand profiles, summary metrics (per cubic centimeter) of comparative process efficiency are derived, as shown in figure 5.

Demand profiles A through D reflect situations of uniform demand, in which the number demanded of each type is equal (see table 3). Demand profiles E through G demonstrate how changes to the mix of parts in the build volume affect production cost, even if the criterion of technical efficiency is satisfied. The main insight won from the demand profiles A, B, and C is that production quantity is only an indirect determinant of manufacturing costs and energy consumption. Ruffo and Hague (2007) argue that increases in production quantity diminish the average cost by enlarging the allocation base for the total cost of the build. In contrast, this work argues that not unused capacity, but the ability of the AM user to fill the available build volumes drives manufacturing costs.

The results for the other three demand profiles leading to technically efficient builds—E, F, and G—show that changes in the part mix create an unpredictable effect on the efficiency of the investigated AM process. It appears that some part

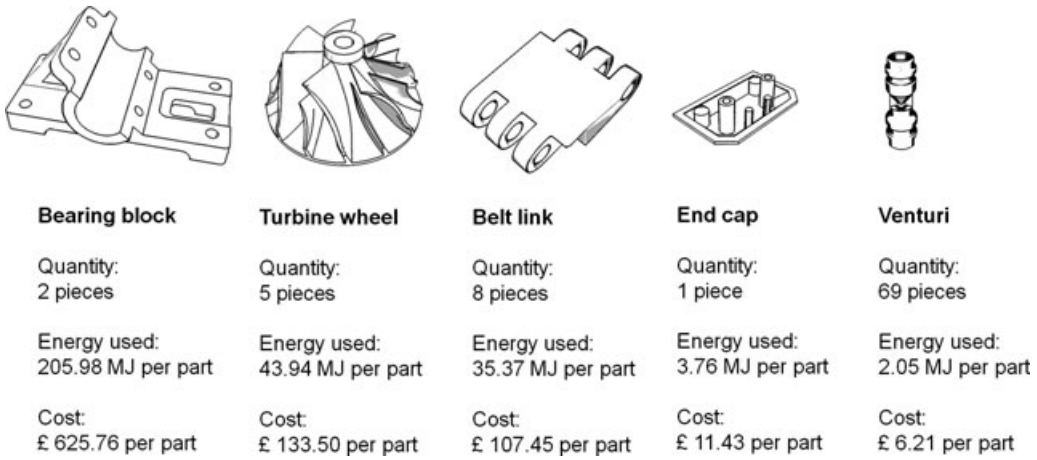

Figure 4 Process energy consumption and cost by part, with costs in pounds sterling (£) and energy in megajoules (MJ).

mixes will idiosyncratically lead to more efficient builds than others.

In terms of energy consumption, specification A is the most efficient, despite profile G exhibiting a higher build volume voxel utilization metric (97.53%, table 3). Though not by a wide margin, profile A is also the most cost-effective configuration (570.69 pence/cm^3 versus 571.15 pence/cm^3 in profile F). This indicates that builds with a wide variety of parts are likely to lead to improved process economics through the AM user's increased ability to compose builds freely.

Conclusion

The current research has shown that the one-stop nature of AM can make the monetary and energy flows during the production of complex components strikingly transparent. Thus the adoption of AM also simplifies measurement of the manufacturing energy consumption for life cycle inventory assessments.

Problems arising from AM's parallel nature in the estimation of manufacturing energy consumption and costs have also been discussed, demonstrating that the implementation of an estimation tool that is in harmony with the requirement of efficient technology utilization is viable. As the motivation to measure and reduce energy inputs to production processes is increasing with energy prices (Herrmann and Thiede 2009), this is seen as a very relevant result for potential AM technology adopters.

In many traditional supply chains, where reliable estimates of cumulative energy consumption may be unavailable, the adoption of AM allows producers to provide their customers with

Table 3 Different demand profiles and realized part quantities

	Quantity of parts demanded						
Demand profile	*Bearing block*	*Turbine wheel*	*Belt link*	*End cap*	*Venturi*	*Build volume floor area occupation (voxels)*	*Description*
A	∞ (2)	∞ (5)	∞ (8)	∞ (1)	∞ (69)	92.59%	Uniform demand, excess
B	5 (2)	5 (5)	5 (5)	5 (4)	5 (5)	79.80%	Uniform demand, high
C	3 (2)	3 (3)	3 (3)	3 (3)	3 (3)	62.27%	Uniform demand, intermediate
D	1 (1)	1 (1)	1 (1)	1 (1)	1 (1)	26.32%	Uniform demand, low
E	∞ (3)	—	—	—	—	50.07%	Excess demand, largest part
F	—	∞ (10)	∞ (13)	—	—	82.37%	Excess demand, medium parts
G	—	—	—	∞ (45)	∞ (100)	97.53%	Excess demand, small parts
H	1 (1)	—	—	—	—	16.69%	Single-part build, bearing block

Notes: Values in parentheses show the actual number of parts inserted by the build volume packing algorithm. ∞ = infinity.

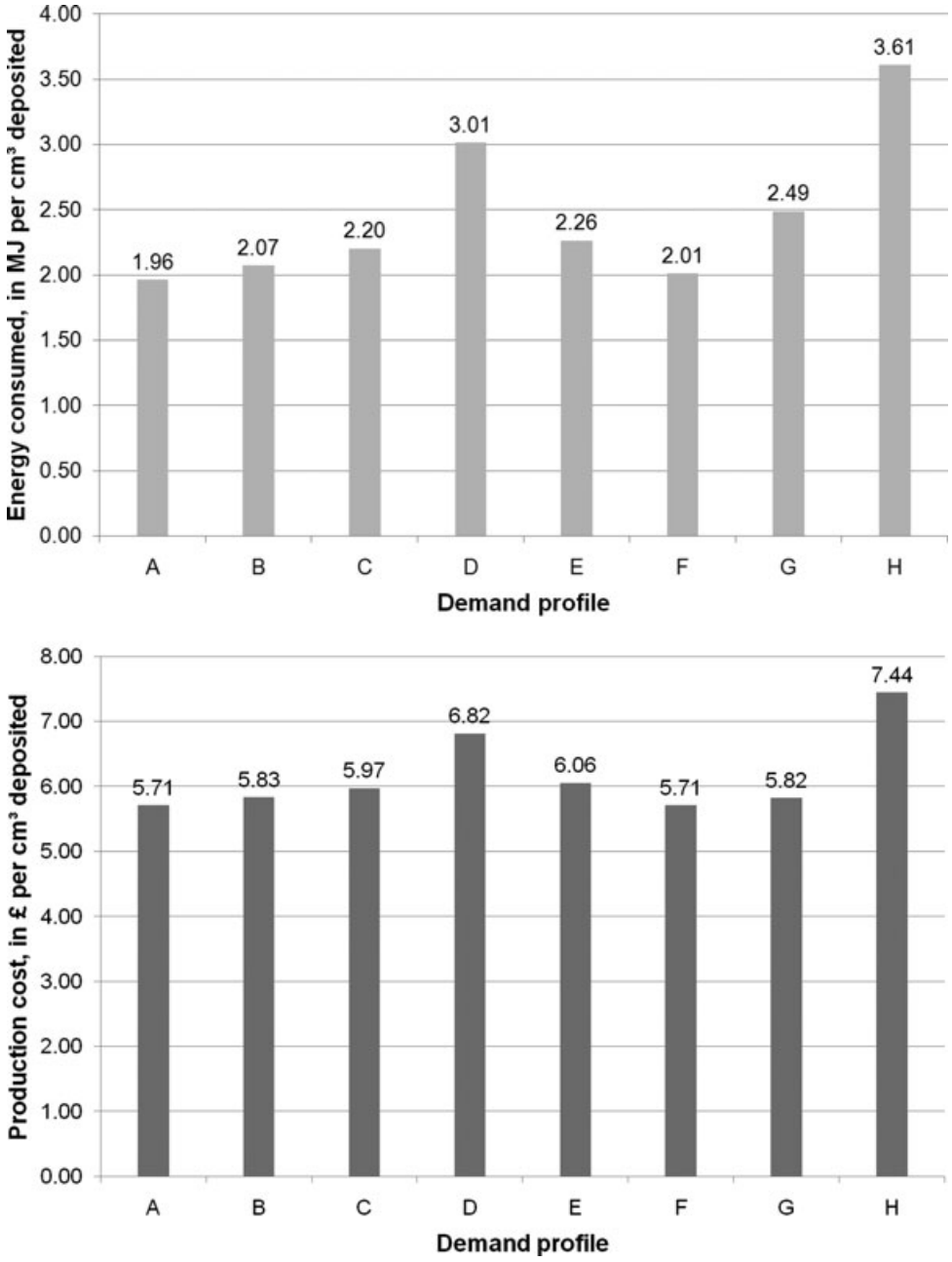

Figure 5 Effect of demand scenario on estimated energy consumption and cost, with dimensions in centimeters (cm), cost in pounds sterling (£), and energy in megajoules (MJ).

reliable data on the energy embedded into products or components during the manufacturing stage. Efforts to reduce the total energy associated with manufacturing using a methodology of "design for energy minimization" are greatly aided by such transparency.

It has been shown that selecting the minimum cost configuration in AM is likely to lead to the secondary effect of minimizing process energy consumption. Hence, from an ecological standpoint, AM adoption may come with the side effect of correcting production configurations featuring non-minimal energy inputs. This aspect may be an important prerequisite for energy efficiency gains in manufacturing (see Lovins 1996). In this context it is important to note that for machining processes (which form an important substitute technology to AM) the cost-minimizing configuration does not necessarily lead to energy consumption minimization (Rajemi et al. 2010).

The corrective described by Lovins is perhaps also a hallmark of a particular class of technology described as "Mumfordian biotechnics." It has been argued that these technologies may in the future replace conventional mass production by a more benign, scalable, and product performance–oriented manufacturing approach (Mumford 1971). Aspects of AM that support

this classification are the qualitative richness of products enabled by AM (Hollington 2008) and the freedom from quantitative pressures associated with the absence of sunk tooling costs present in traditional mass production (Ruffo et al. 2006a).

For a comparison of the environmental impact of AM with those of other manufacturing processes, this article has argued that the impact of manufacturing process choice should not be considered in isolation. It is necessary to explore matching design changes and material selection. These variations are more than likely to impact the environmental performance throughout the life cycle, especially during the use phase. Further research is needed in this area, perhaps in the form of detailed life cycle case studies with combined variation of manufacturing process, design, and material.

Acknowledgements

The authors greatly acknowledge the support given by the technical staff—Roy Darlington, Tony Galley, and Tim Bloor—at the Crewe (UK) facility of Bentley Motors Ltd. Further, the authors greatly acknowledge the support given by Mark Hardy at the Additive Manufacturing Research Group at Loughborough University.

Notes

1. One watt (W, SI) ≈ 3.412 British Thermal Units (BTU)/hour ≈ 1.341×10^{-3} horsepower (HP).
2. One millimeter (mm) = 10^{-3} meters (m, SI) ≈ 0.039 inches.
3. One kilogram (kg, SI) ≈ 2.204 pounds (lb).
4. One kilowatt (kW) ≈ 56.91 British thermal units (BTU)/minute ≈ 1.341 horsepower (HP).
5. One cubic centimeter (cm^3) = 10^{-6} cubic meters (m^3, SI) ≈ 0.0610 cubic inches ($in.^3$). One megajoule (MJ) = 10^6 joules (J, SI) ≈ 239 kilocalories (kcal) ≈ 948 British thermal units (BTU).
6. One gram (g) = 10^{-3} kilograms (kg, SI) ≈ 0.035 ounces (oz).

References

Alexander, P., S. Allen, and D. Dutta. 1998. Part orientation and build cost determination in layered manufacturing. *Computer-Aided Design* 30(5): 343–356.

ASTM. 2010. ASTM F2792 – 10e1 standard terminology for additive manufacturing technologies. www.astm.org/Standards/F2792.htm. Accessed 4 October 2010.

Baumers, M., C. Tuck, R. Hague, I. Ashcroft and R. Wildman. 2010. A comparative study of metallic additive manufacturing power consumption. Paper presented at the 2010 Solid Freeform Fabrication Symposium, 9–11 August, Austin, TX, USA.

Baumers, M., C. Tuck, and R. Hague. 2011. Realised levels of geometric complexity in additive manufacturing. *International Journal of Product Development* 13(3): 185–203.

Boothroyd, G., P. Dewhurst and W. Knight. 1994. *Product design for manufacture and assembly*. New York, NY, USA: Marcel Dekker.

British Standards Institution. 2011. Guide to PAS2050:2011. www.bsigroup.com/en/Standards-and-Publications/Industry-Sectors/Energy/PAS-2050. Accessed 15 May 2012.

Byun, H. and K. H. Lee. 2006. Determination of the optimal build direction for different rapid prototyping processes using multi-criterion decision making. *Robotics and Computer-Integrated Manufacturing* 22(1): 69–80.

Campbell, I., J. Combrinck, D. De Beer, and L. Barnard. 2008. Stereolithography build time estimation based on volumetric calculations. *Rapid Prototyping Journal* 14(5): 271–279.

Choi, S. H. and S. Samavedam. 2002. Modelling and optimisation of rapid prototyping. *Computers in Industry* 47(1): 39–53.

Cormier, D., H. West, O. Harryson, and K. Knowlson. 2004. Characterization of thin walled Ti-6Al-4V components produced via electron beam melting. Paper presented at the 2004 Solid Freeform Fabrication Symposium, 2–4 August, Austin, TX, USA.

DECC (Department of Energy and Climate Change). 2010. Quarterly energy prices, December 2010. www.decc.gov.uk/assets/decc/Statistics/publications/prices/1085-qepdec10.pdf. Accessed 10 May 2011.

Di Angelo, L. and P. Di Stefano. 2011. A neural network-based build time estimator for layer manufactured objects. *International Journal of Advanced Manufacturing Technology* 57(1): 215–224.

Dietmair, A. and A. Verl. 2009. Energy consumption forecasting and optimization for tool machines. *MM Science Journal* March: 62–66.

Else, P. and P. Curwen. 1990. *Principles of microeconomics*. London, UK: Unwin Hyman.

EOS GmbH. 2010. Products. www.eos.info/en/products.html. Accessed 24 September 2010.

Foran, B., M. Lenzen, C. Dey, and M. Bilek. 2005. Integrating sustainable chain management with triple bottom line accounting. *Ecological Economics* 52(2): 143–157.

Gößling-Reisemann, S. 2008. What is resource consumption and how can it be measured? Theoretical considerations. *Journal of Industrial Ecology* 12(1): 10–25.

Gutowski, T., J., Dahmus, and A. Thiriez. 2006. Electrical energy requirements for manufacturing processes. Paper presented at the 13th CIRP International Conference on Life Cycle Engineering, 31 May–2 June, Leuven, Belgium.

Hague, R., S. Mansour, and N. Saleh. 2004. Material and design considerations for rapid manufacturing. *International Journal of Production Research* 42(22): 4691–4708.

Herrmann, C. and S. Thiede. 2009. Process chain simulation to foster energy efficiency in manufacturing. *CIRP Journal of Manufacturing Science and Technology* 1(4): 221–229.

Herzog, T. 2009. World greenhouse gas emissions in 2005. http://pdf.wri.org/working_papers/world_greenhouse_gas_emissions_2005.pdf/. Accessed 15 July 2011.

Hollington, G. 2008. Design 2.0. www.tctmagazine.com/library/115/Design%202.0.pdf. Accessed 18 May 2011.

Hopkinson, N. and P. Dickens. 2003. Analysis of rapid manufacturing—Using layer manufacturing processes for production. *Proceedings of the Institution of Mechanical Engineers, Part C: Journal of Mechanical Engineering Science* 217(1): 31–39.

Hur, S., K. Choi, S. Lee, and P. Chang, 2001. Determination of fabricating orientation and packing in SLS process. *Journal of Materials Processing Technology* 112(1): 236–243.

Ikonen, I., W. E. Biles, A. Kumar, R. K. Ragade, and J. C. Wissel. 1997. A genetic algorithm for packing three-dimensional non-convex objects having cavities and holes. *Proceedings of the 7th International Conference on Genetic Algorithms: Michigan State University, East Lansing, MI, July 19–23*. Waltham, MA, USA: Morgan Kaufmann, 591–598.

Jeswiet, J. and S. Kara. 2008. Carbon emissions and CESTM in manufacturing. *CIRP Annals—Manufacturing Technology* 57(1): 17–20.

Jiménez-González, C. and M. Overcash. 2000. Energy sub-modules applied in life-cycle inventory of processes. *Clean Products and Processes* 2(1): 57–66.

Jovane, F., H. Yoshikawa, L. Alting, C. R. Boër, E. Westkämper, D. Williams, M. Tseng, G. Seliger, and A. M. Paci. 2008. The incoming global technological and industrial revolution towards competitive sustainable manufacturing. *CIRP Annals—Manufacturing Technology* 57(2): 641–659.

Kara, S. and W. Li. 2011. Unit process energy consumption models for material removal processes. *CIRP Annals—Manufacturing Technology* 60: 37–40.

Kellens, K., W. Dewulf, M. Overcash, M. Hauschild, and J. R. Duflou. 2012. Methodology for systematic analysis and improvement of manufacturing unit process life cycle inventory (UPLCI)—CO2PE! initiative (cooperative effort on process emissions in manufacturing). Part 1: Methodology description. *International Journal of Life Cycle Assessment* 17: 69–78.

Kellens, K., E. Yasa, W. Dewulf, and J. R. Duflou. 2010. Environmental assessment of selective laser melting and selective laser sintering. Paper presented at Going Green – CARE INNOVATION 2010: From Legal Compliance to Energy-efficient Products and Services, 8–11 November, Vienna, Austria.

Lovins, A. B. 1996. Negawatts—Twelve transitions, eight improvements and one distraction. *Energy Policy* 24(4): 331–343.

Mazzioli, A., M. Germani, and R. Raffaeli. 2009. Direct fabrication through electron beam melting technology of custom cranial implants designed in a PHANToM-based haptic environment. *Materials and Design* 30(8): 3186–3192.

Mognol, P., D. Lepicart, and N. Perry. 2006. Rapid prototyping: Energy and environment in the spotlight. *Rapid Prototyping Journal* 12(1): 26–34.

Morrow, W. R., H. Qi, I. Kim, J. Mazumder, and S. J. Skerlos. 2007. Environmental aspects of laser-based and conventional tool and die manufacturing. *Journal of Cleaner Production* 15(10): 932–943.

Morrow, W. R., H. Qi, I. Kim, J. Mazumder, and S. J. Skerlos. 2004. Laser-based and conventional tool and die manufacturing: Comparison of environmental aspects. *Proceedings of the Global Conference on Sustainable Product Development and Life Cycle Engineering*, 29 September–1 October, Berlin, Germany, 103–110.

Mumford, L. 1971. *The myth of the machine—The Pentagon of power*. London, UK: Secker & Warburg.

Munguia, F. J. 2009. RMADS: Development of a concurrent rapid manufacturing advice system. Ph.D. thesis, Universitat Politecnica de Catalunya, Barcelona, Spain.

Nyaluke, A., B. Nasser, H. R. Leep, and H. R. Parsaei. 1996. Rapid prototyping work space optimization. *Computers & Industrial Engineering* 31(1/2): 103–106.

Pham, D. T. and X. Wang. 2000. Prediction and reduction of build times for the selective laser sintering process. *Proceedings of the Institution of Mechanical Engineers Part B* 214: 425–430.

Rajemi, M. F., P. T. Mativenga, and A. Aramcharoen. 2010. Sustainable machining: Selection of optimum turning conditions based on minimum energy considerations. *Journal of Cleaner Production* 18(10–11): 1059–1065.

Ruffo, M. and R. Hague. 2007. Cost estimation for rapid manufacturing—Simultaneous production of mixed components using laser sintering. *Proceedings of IMech E Part B: Journal of Engineering Manufacture* 221(11): 1585–1591.

Ruffo, M., C. Tuck, and R. Hague. 2006a. Cost estimation for rapid manufacturing—Laser sintering production for low to medium volumes. *Proceedings of IMech E Part B: Journal of Engineering Manufacture* 220(9): 1417–1427.

Ruffo, M., C. Tuck, and R. Hague. 2006b. Empirical laser sintering time estimator for Duraform PA. *International Journal of Production Research* 44(23): 5131–5146.

Sarwar, M., M. Persson, H. Hellbergh, and J. Haider. 2009. Measurement of specific cutting energy for evaluating the efficiency of bandsawing different workpiece materials. *International Journal of Machine Tools and Manufacture* 49: 958–965.

Son, Y. K. 1991. A cost estimation model for advanced manufacturing systems. *International Journal of Production Research* 29(3): 441–452.

Strutt, P. R. 1980. A comparative study of electron beam and laser melting of M2 tool steel. *Materials Science and Engineering* 44(1): 239–250.

Taylor, P. 2008. Energy technology perspectives 2008—Scenarios and strategies to 2050. Paper presented at the Institute of Energy Economics Workshop, 7 July, Tokyo, Japan.

Telenko, C., C. C. Seepersad, and M. E. Webber. 2008. A compilation of design for environment principles and guidelines. Paper presented at the ASME 2008 International Design Engineering Technical Conferences & Computers and Information in Engineering Conference, 3–6 August, New York, NY, USA.

Tuck, C., R. Hague, and N. Burns. 2007. Rapid manufacturing: impact on supply chain methodologies and practise. *International Journal of Services and Operations Management* 3(1): 1–22.

Tuck, C., R. Hague, M. Ruffo, M. Ransley, and P. Adams. 2008. Rapid manufacturing facilitated customization. *International Journal of Computer Integrated Manufacturing* 21(3): 245–258.

Vijayaraghavan, A. and D. Dornfeld. 2010. Automated energy monitoring of machine tools. *CIRP Annals—Manufacturing Technology* 59(1): 21–24.

Westkämper, E., L. Alting, and G. Arndt. 2000. Life cycle management and assessment: Approaches and visions towards sustainable manufacturing (keynote paper). *CIRP Annals—Manufacturing Technology* 49(2): 501–526.

Wilson, J. O. 2006. Selection for rapid manufacturing under epistemic uncertainty. Master's thesis, Georgia Institute of Technology, Atlanta, GA, USA.

Wodziak, J. R., G. M. Fadel, and C. Kirschman. 1994. A genetic algorithm for optimizing multiple part placement to reduce build time. *Proceedings of the 5th International Conference on Rapid Prototyping*: 201–210. University of Dayton Research Institute, Dayton, OH.

About the Authors

Martin Baumers is a doctoral researcher, **Chris Tuck** is a senior lecturer, **Ricky Wildman** is a professor, **Ian Ashcroft** is a professor, **Emma Rosamond** is a lecturer, and **Richard Hague** is a professor, all at Loughborough University, Loughborough, UK.